February 2007

Dynamically Optimal Strategy to Manage Resistance to Genetically Modified (GM) Crops

Fangbin Qiao, James Wilen and Scott Rozelle

Department of Agricultural and Resource Economics, University of California, Davis, One Shields Avenue, Davis, California 95616. James Wilen and Scott Rozelle are members of the Giannini Foundation.

Correspondence should be addressed to Fangbin Qiao:
Tel: 1-510-524-1532
Email: qiao@primal.ucdavis.edu

Authors note: The authors are grateful to the staff of the Center for Chinese Agricultural Policy who worked so hard in collecting data. We would like to thank Kongming Wu, director of the Institute of Plant Protection, Chinese Academy of Agricultural Sciences; Ruifa Hu, research fellow, Center for Chinese Agricultural Policy, Chinese Academy of Sciences; and Siwa Msangi, Environment and Production Technology Division, International Food Policy Research Institute for their comments. Additionally, the authors acknowledge the financial support of the Economy and Environment Program for Southeast Asia (EEPSEA) and National Science Foundation of China (70021001 and 70333001).

Dynamically Optimal Strategy to Manage Resistance to Genetically Modified (GM) Crops

Abstract

This paper uses a simple model of evolution of pest population and pest resistance to characterize the socially optimal refuge strategy to manage pest's resistance to genetically modified (GM) crops. The technical part of this paper extends previous theoretical economic analyses of treatment by addressing the optimal path to the equilibrium. In this study, we not only show, using detailed theoretical analyses of the characteristics of the steady state, but also analytically and numerically results characterizing the optimal control paths that lead to the final equilibria. We also study the initial circumstances under which a synthesized interventionist control is optimal and the initial circumstances under which an ecological control (zero control) is optimal.

***Key words*:** biotechnology, Bt cotton, resistance, natural refuge crops, Asia, China

Dynamically Optimal Strategy to Manage Resistance to Genetically Modified (GM) Crops

Introduction

The development of genetically modified (GM) crops has been the most successful application of agricultural biotechnology research to date. The main commercialized varieties, *Bacillus thuringiensis* (Bt) transgenic crops, derive their resistance from the insecticide expressed by the gene of the bacterium Bt that is inserted into the DNA of the host crop. Even though cotton and maize engineered with such genes were grown commercially for the first time in 1996, their use has spread very quickly all over the world. In 2004, the total planting area of Bt maize and Bt cotton is 23 million hectares in the world (James, 2005). In addition, James's report predicts that Bt crops as well as other GM crops will be planted on more arable land and in more countries in the future.

The development of biotechnology also has spurred interest in resistance management in recent years. The biotechnologies are also two-edged swords. Even though biotechnology represents the cutting edge of efforts to increase agricultural productivity as well as the improvement of environmental conditions, it also has given rise to a number of concerns. One of the major worries lurking behind this success is the potential vulnerability of GM crops to adaptation by pests. As resistance builds up, the GM crops will lose their efficiency in controlling the pests. In order to control the buildup of resistance in the pest population, a refuge strategy is suggested and applied in almost all the countries where GM crops are planted. Refugia reduce the rate of resistance evolution by allowing insects, which are susceptible to toxins not used in the refuge, to survive and reproduce successfully, thereby reducing the percentage of potentially resistant insects in the overall population. Even though refuge strategy is a commonsense, appreciate refuge requirements remain a matter of debate

because of uncertainty regarding levels of genetic and biological parameters used to simulate resistance evolution and uncertainty regarding models used to estimate the costs and benefits of managing resistance with refugia. Consequently, an interest in searching for an optimal refuge strategy has arisen (Gould, 1998; Hurley et al., 2001; Livingston et al., 2002; Laxminarayan and Simpson, 2002).

The current literature on the design of a refuge strategy to manage the resistance of a pest population to GM crops can be divided into two types. The main objective of the first type study seeks, above all, to determine an optimal refuge size that preserves a pest's susceptibility (henceforth, called biological models). A good example of a biological model is Gould (1998). The other type of study, while also concerned about the buildup of resistance, is more concerned about doing so in a way that maximizes the benefits provided by GM crops to producers (henceforth, called economic models). Among the most notable papers that have dealt with the economic considerations of an optimal refuge strategy to manage Bt crop resistance have been those of Hurley et al. (2001), Livingston et al. (2002), and Laxminarayan and Simpson (2002).

Gould (1998) was one of the first entomologists to examine optimal refuge size using a biological model. In order to preserve the insect population's susceptibility, entomologists try to determine ways to minimize the share of the population of pests that have the resistant genes. Gould's research tried to determine a level such that the part of the population that is resistant to a toxin is small enough that it does not become dominant in the population for some specified length of time. The biological objective is to try to ensure that the population will not evolve into one that is uncontrollable by the GM toxin. By using a population genetics model, Gould (1998) shows that in order to keep the fraction of the resistant pests below a goal of 0.10 over a 10 year span, the effective non-spray refuge size needs to be larger than the current requirements of 4%.

Hurley and his colleagues (Hurley et al., 1997 and 2001; Secchi et al., 2001) were among the first research team to set up economic models that seek to estimate an optimal refuge strategy for the management of a pest population's resistance to GM crops. The shortcoming of biological models is that they ignore the economic tradeoffs between the pest control and population management benefits and costs of transgenic varieties. Economists have pointed out that even though the establishment of refuges for pests helps to preserve the pest's susceptibility to the toxins expressed by the GM crops, maintaining susceptibility can be costly. If the cost is too high, it may be that the benefits from the adopting refuge strategy are not substantial enough to offset the costs. Numerically, Hurley and colleagues show that the benefit of maize production can be maximized with a 10.6% non-Bt maize refuge size which is smaller than the required 20% by the United States Environmental Protection Agency (EPA). Empirical studies by Livingston et al. (2000 and 2002) found a similar set of results for the case of Bt cotton in the United States. Both sets of results assume fixed pest resistance and are derived with models that are static.

The work of Laxminarayan and Simpson (2000 and 2002) goes one step further than the previous studies that use economic models. Using an analytical model that incorporates the evolution of pest populations and pest resistance buildup, Laxminarayan and Simpson characterize the socially optimal refuge strategy for managing pest resistance to GM crops. There results are derived within a dynamic modeling framework, but they characterize solutions only in terms of steady state solutions. The second contribution of Laxminarayan and Simpson is that they show both that the establishment of refuge areas might best be delayed until resistance becomes an important concern, and that the use of refuge areas in the long run will not be optimal under some circumstances (i.e. the fitness cost of resistance does not exceed the discount rate). While an important extension of the literature, the shortcoming of Laxminarayan and Simpson's paper is that it lacks an analysis of the optimal *path* of refuge,

which is an important feature of an optimal refuge strategy.

The bioeconomic model we use as a foundation for our analysis follows from the epidemiological model in Wilen and Msangi (2002). However, the model we present is not only an application of Wilen and Msangi's model in the case of GM crops, but also a generalization in several directions. The first important generalization is the detailed analysis of the characteristics of the steady states. Wilen and Msangi did solve for the steady states, however, they did not focus on the analytical discussion of the characteristics of the steady states. In this study, we discuss in detail the nature of all the steady states, their stability properties, and circumstances under which these steady states will emerge as long run solutions to the dynamic problem.

Our second contribution is to explore the importance of the impact of fitness cost on an optimal refuge strategy. Wilen and Msangi generalize the zero fitness cost assumption in Laxminarayan and Brown's model, but they focus on the differences between zero fitness cost and non-zero fitness cost. We generalize the impact of fitness cost on optimal treatment strategy by exploring how the qualitative properties of optimal solutions depend upon the size of fitness costs. We numerically show that relatively low fitness cost makes the solution qualitatively like that of a non-renewable resource problem, in the sense that the decision is mainly one of determining how fast to dissipate a valuable stock, namely the stock of susceptible pests. In contrast, we show that relatively high fitness cost makes the problem more like a renewable resource problem in which the main decision concerns the steady state level that the stock of susceptible pests ought to be driven to.

The remainder of this paper is organized as follows. We introduce our model in section 2. Analysis of our bioeconomic model shows that the under different circumstances, the dynamic optimal refuge strategy is also different. For some initial conditions where the pest population and/or the fraction of susceptible pests are high, the dynamically optimal

refuge strategy is a combination of the extreme control and a singular control that will drive the whole system into a final equilibrium. For other circumstances with different initial points, no control (or rather, a zero control) is optimal. In Section 3, we develop a discretized form of our bioeconomic model to check these theoretical results. Results of the numerical simulation of our model are consistent with our theoretical analysis. Section 4 concludes the paper.

The Bioeconomic Model

The integrated bioeconomic model that we use follows the epidemiological model presented by Wilen and Msangi (2002). A similar approach is used in the models presented by Laxminarayan and Simpson (2002), Hurley et al. (2001) and Livingston et al. (2002) in their studies on refuge strategies. The pest population is assumed to be local (that is, both in- and out-migration is ruled out). We also use other standard assumptions implicit in deriving the Hardy-Weinberg principle, such as random mating between resistant and susceptible pests, negligible mutation, non-overlapping pest generations and the sexual reproduction of pests. The model consists of two parts: a biological model which is used to simulate the evolution of pest resistance; and a dynamic regulatory model which is used to examine the impact of refuge policies. Because the regulatory model is easier to describe once the biological model is understood, we begin with the biological model.

Biological Model

The pest population is denoted by D. A number of biological models assume that the pest population grows logistically (see, e.g. Clark 1976). Following the assumption of these studies, we shall assume that the pest population grows logistically with an intrinsic growth rate of g, and a carrying capacity per unit of land normalized to 1. Total land is assumed to be fixed, and is normalized to 1. The total number of new pest organisms hatched (presuming them to be the offspring of egg-bearing insects) in every period is given by gD(1-D). From

this gross addition, we must subtract to account for mortality among pests.

The pest population is divided among "susceptible" and "resistant" organisms. The former will be assumed to die with a high mortality rate, h, if treated and a zero mortality rate if not. The mortality rate of the resistant organisms is assumed to be r, which is also known as the fitness cost, regardless of whether the pest is treated or not. We assume that a fraction, w, of all pests is susceptible to the toxin, and the remaining fraction 1-w is immune. A refuge strategy calls for planting a fraction, q, of the total land devoted to agriculture in the GM crop. Hence, the fraction 1 – q of agricultural land will be devoted to a non-GM variety. As shown in Appendix 1, the dynamics of the pest population and the fraction of the susceptible pests are given by:

$$\frac{dD}{dt} = gD(1-D) - qwhD - (1-w)rD$$

$$\frac{dw}{dt} = (qh - r)w(w-1) \qquad (1)$$

Regulatory Model

The objective economic function is to minimize the discounted sum of treatment costs (cost of planting GM crops) and damage costs as a result of pests. The dynamic model system can be stated as follows:

$$\min_{0 \le q \le 1} \int_0^{\infty} [\alpha * D + c * q] * e^{-\rho t} \, dt$$

$$\text{s.t.} \quad \frac{dD}{dt} = gD(1 - D) - qwhD - (1-w)rD$$

$$\frac{dw}{dt} = (qh - r)w(w-1) \qquad (2)$$

where α is the average damage cost per unit of the normalized pest population; c is the average additional cost associated with GM crop planting; and ρ is the discount rate. The

control variable in Equation (2) is the fraction of GM crop, q. And the two state variables are the total pest population (D) and the fraction of the susceptible pests (w). The fraction of agricultural land set aside as refuge area in each period (1-q) determines the cost in each period, as well as the effectiveness of the GM crop against pests in the subsequent periods. There is, then, an inter-temporal tradeoff between crop losses today and more rapidly eroding toxic effectiveness in the future.

Unfortunately, as shown in Appendix 2, the second-order necessary conditions for a minimum of the Hamiltonian do not hold for this type of problem. The corresponding current value Hamiltonian is:

$$H(.) = \alpha * D + c * q + \lambda[gD(1- D) - wqhD - (1-w)rD] + \mu(qh - r)w(w-1) \qquad (3)$$

and it is not globally convex, as is necessary to conclude that the solution is a global minimum. As a consequence in the following section, we solve the system for some equilibria that may only be local minima. In this sense, these equilibria are called "potential steady states" (See Appendix 3). This inability to identify global minimizing equilibria seems to be a feature of these kinds of models, and is found, for example, in Gersovitz and Hammer (2004).

Optimal Control Strategies

The Hamiltonian is minimized in each period with an appropriate choice of the optimal fraction of GM crop, q. Since this problem is linear in the control variable, we need to isolate the switching function, which is $\sigma(t) = c - \lambda whD + \mu wh(w-1)$. The switching function is a coefficient in the Hamiltonian that multiplies the control variable and hence measures the marginal addition to costs that are contributed per unit of the control variable. As can be seen, the switching function is time dependent, and it depends upon both state variables and shadow values. Here λ and μ are the shadow values of the size of the total pest population and the population that is made up of susceptible pests. In a traditional resource problem (which typically is seeking to maximizing the value of return-based activities), the

shadow price of the pest population is negative since the pest population is a "bad" resource. In our study, however, since the objective is to minimize the cost function, a large pest population will contribute to higher costs, so λ can be defined as positive. For a similar reason, μ can be viewed as negative instead of positive as in a traditional resource problem.

The sign of the switching function determines the choice of the treatment. The switching function is the coefficient of the control, and the Pontryagin optimality conditions state that:

$$\begin{aligned} q &= 0 \quad \text{if} \quad \sigma(t) > 0 \\ q &= q^* \quad \text{if} \quad \sigma(t) = 0 \\ q &= 1 \quad \text{if} \quad \sigma(t) < 0 \end{aligned} \tag{4}$$

When the switching function is negative, all of the land should be planted with GM crop (or q=1) to minimize the Hamiltonian. And when the switching function is positive, all of the land should be planted to the non-GM crop. When the switching function is zero, however, a so-called singular path is followed. The singular control may be complicated and time varying, and it must be determined using additional computations that hold along an optimal path. As in Wilen and Msangi (2002), the complete solution to a linear control problem generally involves a "synthesized" control that consists of segments of extreme controls, followed by segments of singular controls.

The choice of treatment also affects the value of the switching function as the dynamics unfold and change relative values of the state and shadow variables. For example, if the switching function is negative initially, then a maximum control is used to minimize the Hamiltonian. With the use of the maximum treatment, the total pest population and the fraction of the susceptible pests will decrease. Consequently, both the shadow prices of the total pest population and the susceptible pests will also change. These factors, working together, will change the value of the switching function. And if the sign of the switching

function changes from negative to positive, the optimal treatment will change from maximum control (q=1) into minimum control (q=0). In other words, choice of treatment will also change the value of the switching function, which in turn will influence future optimal values of the treatment.

There are three possibilities for sign regimes of the switching function along the optimal path. First, the sign of the switching function may not change and remain always negative up to and until the final equilibrium is arrived at. The second possibility is that the sign of the switching function may not change and always remain positive. The third possibility is that the sign of the switching function may change (possibly multiple times) along the optimal path, either from positive to negative or vice versa. Each of these possibilities will be associated with a qualitatively and quantitatively different optimal control path and a different final equilibrium.

An extreme maximum control will be optimal if the switching function is always negative along the control path. As discussed above, as the maximum treatment is adopted, the system dynamics will cause the magnitude of the switching function to change. However, these changes may not lead to a change in the **sign** of the switching function. If the switching function is always negative, even though it is becoming larger and larger, the optimal choice is still to always use maximum treatment to minimize the Hamiltonian. If this policy is used throughout the whole program, the fraction of the susceptible pest population will be driven towards zero and the total pest population will return to a high level less than the natural equilibrium.

Similarly, a zero control (no Bt planting) will be optimal if the switching function is always positive along the control path. If the switching function does not change sign before the equilibrium arrives, the second possibility is that the switching function is always positive throughout the whole program. . In this case, a zero control will lead the system back to the

natural equilibrium in which both the fraction of the susceptible pests and the total pest population levels are at their maximum levels.

A synthesized control that consists of segments of extreme control and singular control is optimal if the switching function changes sign along the control path. As discussed above, the sign of the switching function determines the treatment, and the treatment also impacts the magnitude of the switching function. Consequently, along the control path, the switching function may change signs, either from negative to positive or vice versa. Under this situation, the optimal treatment strategy is a combination of extreme control (maximum if the sign of the switching function is negative or/and minimum if the sign of the switching function is positive) and a possibly singular path that will drive the whole system into equilibrium. In Appendix 3, we solve for the singular control and prove that the equilibrium approached by the singular path is a saddle point.

Numerical Simulations of the Model

To check these qualitative predictions and perform comparative dynamics experiments, we develop a discretized form of this problem that can be solved with Dynamic Programming methods. We can optimize this problem by using the Bellman Equation, which can be written as:

$$\underset{0\le q\le 1}{Min} V(D_t) = D_t\alpha + cq + \delta V(D_{t+1})$$

$$\text{s.t.} \quad D_{t+1} - D_t = gD_t(1-D_t) - w_t q_t h D_t - (1-w_t) r D_t, D_{t=0} = D_0$$

$$w_{t+1} - w_t = (q_t h - r) w_t (w_t - 1), w_{t=0} = w_0 \qquad (5)$$

where the function $V(D_{t+1})$ gives the carry-over cost from one period (t) to the next (t+1) of the residual pest population level, which we also seek to minimize and discount with the factor $\delta = 1/(1+\rho)$. The optimal solution of the Bellman equation in each period is

equivalent to the optimal solution of the continuous time control problem for the corresponding periods, by Bellman's principle of optimality. We iterate to find a polynomial approximation to the value function $V(D_{t+1})$ and then use it to solve the Bellman equation forward for each period. We employ a Chebychev polynomial approximation algorithm to solve for the value function, which was easily implemented in GAMS. A good discussion of approximation methods is given by Kenneth Judd (Judd, 1998).

Table 1 reports the defaults values and resources of the economic and biological parameters that we use in the simulation model. The data that form the base for this study are from a dataset collected by the Center for Chinese Agricultural Policy of the Chinese Academy of Sciences in the Yellow River cotton production region. The Yellow River Valley is the largest cotton production region in China and it is also the region where cotton bollworm is most serious. The economic parameters used in this study are based on these empirical data. The biological parameters (i.e. the mortality rates of the pests) come from previous studies and data that were collected by scientists from the Institute of Plant Protection of the Chinese Academy of Agricultural Sciences in their laboratories and during their fieldwork. A detailed discussion about the economic parameters and biological parameters is given in another paper (Qiao, 2006).

The simulation results demonstrate that the qualitative nature of the optimal dynamic refuge strategy to manage the pest's resistance depends importantly on whether the fitness cost is high or low (Figure 1). Recall that fitness cost is the extra mortality that a pest endures if it has the gene that allows it to be resistant to Bt toxin. Consider first the case when fitness cost is low (Panel A), so that there is no mortality penalty associated with being resistant to Bt toxin. Then the consequences of using Bt to control a pest population will be an inevitable loss of the stock of susceptible pests and the main decision is how fast to dissipate this value stock.

This scenario is demonstrated in Panel A. Suppose, to start the simulation, that the initial conditions are characterized by a sudden infestation of a pest, all of which are susceptible to Bt toxins. The optimal solution begins with a phase in which it is optimal to plant the Bt crop on all arable land. Because both the fraction of susceptible pests and the total pest population level are high in the initial period, the marginal payoff to control (planting GM crop) is higher than the payoff of planting non-GM refuge. Consequently, the optimal refuge size is set to zero at the initial periods. This policy continues for several periods, reducing the pest population and associated damages, and as a negative side effect, reducing the population of pests that are susceptible to the toxin. The simulation results demonstrate that planting a refuge initially is not economic. It is not economic, in fact, until the buildup of resistance in the pest population becomes an important concern. This finding is consistent with previous studies (i.e. Laxminarayan and Simpson, 2002).

The second phase exhibits periods of either full control (100% GM crops) or no control. As discussed in the above, the 100% full control in the first phase will continuously increase the value of the switching function. Consequently, the value of the switching function might become positive, in which case in order to minimize the objective function, a zero control, or 100% non-GM crop planting policy, is optimal. Similarly, zero control decreases the value of the switching function, and then, after some period has elapsed, might allow full control to again become optimal if the value switching function change signs. As can be seen in Panel A, the second phases is characterized by "bang-bang" controls in which the optimal decision switches back and forth between extreme controls in response to the sign switches of the switching function. The switching function, of course, is the contribution of a marginal unit of GM crop planting to overall damage and planting costs. During the second phase, the pest population is driven down by the use of Bt cropping, while the stock of susceptible pests also falls in a manner moderated by periodic planting of non-Bt crops. These

phases in which all non-Bt crops are planted are essentially periods of refuge establishment, but global and periodic rather than spatial and permanent.

During the third phase, an oscillating control is followed when the switching function is zero. The oscillation happens because there is only one control variable (Bt planting) to control two state variables (total pest population and proportion susceptible). That is, it is desirable to reduce the total pest population and sustain the susceptible, but the only way to affect those states is via Bt planting. But the single control does not allow smooth and independent control of each state variable separately and the best that can be done is joint control with oscillation into equilibrium. After several sign switches in the second phase, either from positive to negative or from negative to positive, the switching function becomes zero the control locks into a singular path of time-varying interior controls. Detailed discussion of single path and the equilibrium driven by the singular path is shown in Appendix 3. Along the singular path, the switching function stays zero and some non-zero refuge is planted. The oscillating control will lead the whole system into the final equilibrium.

Eventually, the singular path causes the stock of the pest population and the fraction of the susceptible pests to approach a steady state equilibrium. Note that in Panel A, the steady state is one in which the pest population is high and the susceptible population low. This s a characteristic of the low fitness cost case. With low fitness costs, the long run steady state is one where most of the crop land is planted to non-Bt crop and the little Bt that is used is used to keep the pest population only moderately at bay. Most of the activity for this case is focused on getting the pest population and its damages reduced early in the horizon, after which controls are reduced controls are reduced because of the unavoidable buildup of resistant pests

In contrast, suppose that fitness costs are high, as depicted in Panel B of Figure 1. In this case, “nature” helps clear out some of the pests, particularly those bearing the fitness cost

of having a resistance gene to Bt. When fitness costs are high, the optimal dynamic policy is much more straightforward than for the low fitness cost case. In particular, there is no bang-bang switching of controls and no oscillation into an equilibrium. In this case, the higher natural mortality experienced by resistant pests helps drive their numbers and the total pest population to low levels after application of Bt cropping for an initial period. After a (longer) period of Bt planting, the optimal strategy shifts directly into a steady state strategy with partial Bt planting. That interior control of a mixed system is maintained in a long run equilibrium.

The steady state equilibrium with high fitness costs is qualitatively different from the low fitness cost case. In the limiting case of low fitness where there is absolutely no fitness cost to being resistant, the long run outcome is one with a very high pest population, most of which is resistant to Bt, and a low application of Bt cropping. This is the long run consequence of having no other way to deal with the pest population than to control it with Bt, at a cost of permanently building up the resistant pest population. With low fitness costs, the steady state is one in which there is some continual and significant application of Bt technology, a relatively lower overall pest population level, and a lower proportion of resistant pests. In this case, the application of Bt to reduce pests is aided by high natural mortality of resistant pests, and the pest population can be maintained at a lower level for a longer period of time.

The scenarios depicted in Panels A and B in Figure 1 begin with initial conditions depicting an infestation, so that the initial pest population is assumed large. In addition, we must make assumptions about the nature of the initial infestation and particularly its make up with respect to resistant pests. Both of the above cases assume an initial population of pests near its maximum natural carrying capacity level, with virtually all pests susceptible to Bt toxins. But what about other initial conditions? Are the steady states depicted in Figure 1 to

be expected for other initial circumstances? We investigated this by searching for initial condition combinations in which the steady states were not interior as depicted in Figure 1.

As discussed earlier, the qualitatively nature of the control type depends upon the path of the switching function, which is itself endogenous. In the cases in Figure 1 the switching function changes sign at least once. If the switching function does not change sign along the control path, then an extreme control (either full control or zero control) will be optimal. To check whether there are indeed initial circumstances under which the extreme control is optimal, we re-simulated the model, changing only the initial values of the state variables. The results are shown in Figure 2, for the low fitness cost case. Panel A of Figure 2 shows the circumstances under which a synthesized control is optimal, while Panel B shows the circumstances under which extreme control (zero control in this case) is optimal. As shown in Panel B, for some initial values, it is optimal to forego any intervention and control, and instead rely on nature to fight pests. These are conditions under which the pest population is large, but the fraction of susceptible pests is not high. Under this treatment regime, since no control is used, both the pest population and the fraction of the susceptible pests will finally return to their maximums. In Panel A, we show some initial conditions for which the optimal policy is the synthesized control shown in Panel A of Figure 1, namely extreme, bang-bang, oscillation and steady state, ending with a low population of susceptible pests. These circumstances are when the initial pest infestation is high, but the level of susceptible pests is low. The important point is that the optimal strategy for introducing Bt cropping (inherently more expensive) depends upon, in addition to relative costs and damages, the size of the control task as indicated by the nature of the original infestation.

Conclusions

In this paper, we theoretically and numerically analyze the optimal strategy to manage the buildup of resistance in the pest population. The technical part of this paper extends previous theoretical economic analyses of treatment by addressing the optimal path to the equilibrium. In this study, we not only show, using detailed theoretical analyses of the characteristics of the steady state, but also analytically and numerically results characterizing the optimal control paths that lead to the final equilibria. We also study the initial circumstances under which a synthesized interventionist control is optimal and the initial circumstances under which an ecological control (zero control) is optimal.

We believe these results have important qualitative implications for economically optimal GM crop planting strategies. Even though this paper does not exactly mimic the real production environments of GM crops, results from this study at least provide some useful hint about optimal GM crop planting strategies. As shown in the figures, when a GM crop is first introduced in circumstances in which both the pest population and the fraction of the susceptible pests are high, the best choice is to plant 100% GM crop. If we believe a new GM variety or conventional pesticide will be developed in a short run, then planting non-GM crop as a refuge might not be needed. Even if a refuge is needed in the long-term, establishment of the refuges can be delayed until the resistance becomes a real concern.

Qualitative implications of these results are not limited in the management of the GM crops. Even though this study deals directly with the management problem of pesticide resistance to GM crops, the analysis can be used to address other similar questions in biological and medicinal fields, such as antibiotic use in humans, controlling the spread of epidemics, etc. In other words, this analysis contributes understanding to the general resistance management problem.

Acknowledgments

The authors are grateful to the staff of the Center for Chinese Agricultural Policy who worked so hard in collecting data. We would like to thank Kongming Wu, director of the Institute of Plant Protection, Chinese Academy of Agricultural Sciences; Ruifa Hu, research fellow, Center for Chinese Agricultural Policy, Chinese Academy of Sciences; and Siwa Msangi, Environment and Production Technology Division, International Food Policy Research Institute for their comments. Additionally, the authors acknowledge the financial support of the Economy and Environment Program for Southeast Asia (EEPSEA) and National Science Foundation of China (70021001 and 70333001).

Appendix 1. Solving for Equations of Motion

The essentials of the bioeconomic model are captured in the schematic in Figure A1. The pest population is divided into "susceptible" pests (denoted by Ds) and "resistant" pests (denoted by Dr). Since we assume the fraction of the susceptible pests in the total pest population is w, we have Ds=w*D and Dr=(1-w)*D. Similarly, among the total number of the new pests, there are w*g*D*(1-D) susceptible pests and (1-w)*g*D*(1-D) resistant pests separately. From this gross addition, we must subtract mortality among pests. We continue to assume that the total pest population is distributed evenly in the GM and non-GM crop field, so there are q*D pests in the GM crop field and (1-q)*D pests in the refuge. Since the mortality rate of susceptible and resistance pests are h and r separately, there are q*w*h*D susceptible and q*(1-w)*r*D resistant pests dying in the Bt field. Similarly, in the non-GM crop refuge, there are 0 susceptible pests and (1-q)*(1-w)*r*D resistant pests dying.

We must subtract mortality pests from the intrinsic growth rate for both susceptible pest and resistant pests. Then we have an expression for the evolution of the susceptible pests and resistant pests.

$$\frac{dDs}{dt} = wgD(1 - D) - wqhD \qquad \text{(A1-1)}$$

$$\frac{dDr}{dt} = (1\text{-}w)gD(1\text{-}D) - q(1\text{-}w)rD - (1\text{-}q)(1\text{-}w)rD$$

$$= (1\text{-}w)gD(1\text{-}D) - (1\text{-}w)rD \qquad \text{(A1-2)}$$

Consequently, the evolution of the total pests is:

$$\frac{dD}{dt} = \frac{dDs}{dt} + \frac{dDr}{dt} = gD(1\text{-}D) - qwhD - (1\text{-}w)rD \qquad \text{(A1-3)}$$

And the evolution of the fraction of the susceptible pests in the total pest population is:

$$\frac{dw}{dt} = \frac{d(\frac{Ds}{D})}{dt} = [(\frac{dDs}{dt}) * D - Ds*(\frac{dDr}{dt})] / D^2$$

$$= \{[wgD(1-D) - wqhD]*D - wD*[gD(1-D) - wqhD - (1-w)rD]\}/D^2$$

$$= (- wqh) - w[- wqh - (1-w)r]$$

$$= (qh - r)w(w-1) \qquad \text{(A1-4)}$$

Appendix 2. Convexity of the Hessian Matrix of the Hamiltonian

The sufficient conditions to minimize the Hamiltonian is that the Hessian matrix of the Hamiltonian with respect to (q, D, w) must be positive semi-definite. In other words, three types of conditions must be satisfied. First, all the determinants of the three first-order principle minors must be non-negative, or $H_{qq} \geq 0$, $H_{DD} \geq 0$, and $H_{ww} \geq 0$. Secondly, all the determinants of the three second-order principle minors must be non-positive, or

$$\begin{vmatrix} H_{DD} & H_{Dw} \\ H_{Dw} & H_{ww} \end{vmatrix} \leq 0 \qquad \begin{vmatrix} H_{DD} & H_{Dq} \\ H_{Dq} & H_{qq} \end{vmatrix} \leq 0 \qquad \begin{vmatrix} H_{ww} & H_{wq} \\ H_{wq} & H_{qq} \end{vmatrix} \leq 0$$

Finally, the determinant of the third-order principle minors must be non-negative.

$$\begin{vmatrix} H_{DD} & H_{Dw} & H_{Dq} \\ H_{Dw} & H_{ww} & H_{wq} \\ H_{Dq} & H_{wq} & H_{qq} \end{vmatrix} \geq 0$$

In the following, we will check these conditions one by one.

From the Hamiltonian, $H = D^*\alpha + c^*q + \lambda^*dD/dt + u^*dw/dt = D\alpha + cq + \lambda[gD(1-D) - wqhD - (1-w)rD] + \mu(qh - r)w(w-1)$, we get:

$H_{DD} = 2g\lambda$

$H_{Dw} = \lambda^*[- q^*h + r]$

$H_{Dq} = \lambda^*[- w^*h]$

$H_{ww} = 2\mu^*(q^*h - r)$

$H_{qw} = -\lambda^*h^*D + \mu^*h^*(2w-1)$

$H_{qq} = 0$

As discussed above, the shadow price, λ, is positive in this study. So we have:

$H_{DD} = 2g\lambda \geq 0$, $H_{ww} = 0 \geq 0$, $H_{qq} = 0 \geq 0$.

Secondly, these three second-order principle minors are:

$$\begin{vmatrix} H_{DD} & H_{Dw} \\ H_{Dw} & H_{ww} \end{vmatrix} = \begin{vmatrix} 2g\lambda & 0 \\ 0 & 0 \end{vmatrix} = 0 \le 0$$

$$\begin{vmatrix} H_{DD} & H_{Dq} \\ H_{Dq} & H_{qq} \end{vmatrix} = \begin{vmatrix} 2g\lambda & -\lambda wh \\ -\lambda wh & 0 \end{vmatrix} = -(-\lambda wh)^2 \le 0$$

$$\begin{vmatrix} H_{ww} & H_{wq} \\ H_{wq} & H_{qq} \end{vmatrix} = \begin{vmatrix} 0 & -\lambda hD \\ -\lambda hD & 0 \end{vmatrix} = -(-\lambda hD)^2 \le 0$$

Finally, the determinants of the third-order principle minors must be negative, or

$$\begin{vmatrix} H_{DD} & H_{Dw} & H_{Dq} \\ H_{Dw} & H_{ww} & H_{wq} \\ H_{Dq} & H_{wq} & H_{qq} \end{vmatrix} = \begin{vmatrix} 2g\lambda & 0 & -\lambda wh \\ 0 & 0 & -\lambda hD \\ -\lambda wh & -\lambda hD & 0 \end{vmatrix} = -(2g\lambda) * (\lambda hD)^2 \le 0$$

Even though the necessary conditions for the first-order and second-order principle minors are satisfied, the necessary condition for the third-order principle minor does not hold. Consequently, the second order necessary conditions of the minimum do not hold.

Appendix 3 The Optimal Control Path

As discussed in the second section of this paper, there are three possibilities for the sign of the switching function along the optimal path: always negative, always positive, or sometime positive and sometimes negative. In this appendix, we will discuss these three possibilities, characteristics of the fixed points and the optimal control path for each possibility.

A1 Case I – Optimal Full Control

If the switching function is always negative, full control, or q=1, will be used to minimize the Hamiltonian. And at the equilibrium, we should have:

$$\frac{dD}{dt} = gD(1 - D) - qwhD - (1-w)rD = gD(1 - D) - whD - (1-w)rD = 0$$

$$\frac{dw}{dt} = (qh - r)w(w-1) = (h - r)w(w-1) = 0$$

$$\sigma(t) = c - \lambda whD + uhw(w-1) < 0 \qquad \text{(A3-1)}$$

From $\frac{dw}{dt}=0$, we either have $w_1=0$ or $w_2=1$. Plug w=0 into the switching function to get $\sigma(t) = c - \lambda whD + uhw(w-1) = c > 0$, which is contradicted with the negative switching function assumption. Similarly, if we plug w=1 into $\frac{dD}{dt}=0$ to get $D_1=0$ or $D_2=\frac{g-h}{g}$. Using the default value of Appendix Table 1, we have $D=\frac{g-h}{g}<0$, which is not a true solution in practice. Plug w=1 and D=0 to the switching function to get $\sigma(t) = c - \lambda whD + uhw(w-1) = c > 0$, which is contradicted with the negative switching function assumption. In other words, the negative switching function and full control can not be an optimal solution.

A2 Case II – Optimal No Control

If the switching function is always positive, in order to minimize the Hamiltonian, no control is used, or q=0. And at the equilibrium, we should have:

$$\frac{dD}{dt} = gD(1 - D) – qwhD - (1-w)rD = gD(1 - D) - (1-w)rD = 0$$

$$\frac{dw}{dt} = (qh – r)w(w-1) = (– r)w(w-1) = 0$$

$$\sigma(t) = c - \lambda whD + uhw(w-1) > 0 \qquad \text{(A3-2)}$$

Solve for the equation system (A3-2), we get four steady points. They are:

(D=0, w=0)

(D=0, w=1)

(D=$\frac{g-r}{g}$, w=0) and

(D=1, w=1)

In order to analyze the characteristics of these possible steady points, in the following, I will first discuss the characteristics of these four possible steady states by drawing a phase diagram in a (D, w) plane. Then I will check the analytical results using numerical simulations

$$\frac{dD}{dt} = gD(1 - D) – qwhD - (1-w)rD = gD(1 - D) - (1-w)rD$$

$$\frac{dw}{dt} = (qh – r)w(w-1) = (– r)w(w-1) \qquad \text{(A3-3)}$$

First, to solve for the w and D nullclines, we set $\frac{dw}{dt}=0$ and $\frac{dD}{dt}=0$. Solving these two equations yields w=0, w=1, D=0, and D=$\frac{g-r}{g}+\frac{r}{g}w$. These nullclines are plotted in Figure A2, which presents the phase portrait of the dynamic system.

Note that the nullclines divide the phase space into different isosectors. In the following, we will turn to the derivation of the vector field. In other words, we need to figure out the directions of motion for points not on the nullclines. First of all, we take the first derivative of $\frac{dD}{dt}$ with respect to w, and evaluate it at $\frac{dD}{dt}$=0, we get

$$\left.\frac{dD/dt}{dw}\right|_{\frac{dD}{dt}=0} = rD \qquad \text{(A3-4)}$$

So we have $\left.\frac{dD/dt}{dw}\right|_{\frac{dD}{dt}=0}$ >0 when D >0 and $\left.\frac{dD/dt}{dw}\right|_{\frac{dD}{dt}=0}$ <0 when D <0. Sign of $\frac{dD/dt}{dD} = g(1-2D)-(1-w)r$ is positive near (D=0, w=0) and (D=0, w=1). Similarly, $\frac{dw/dt}{dw} = -r(2w-1)$ is positive near (D=0, w=0) and (D=$\frac{g-r}{g}$, w=0), and it is negative near (D=0, w=1) and (D=1,w=1). From these signs, we can determine the direction of motions for points that are not on the nullclines (see Figure A2). In addition, numerical simulation of function A3-3 is consistent with the theoretical analysis above (see Figure A3). In other words, both numerical simulation and analytical discussion show that (D=0, w=0) and (D=0, w=1) are two saddle points, (D=1, w=1) is an asymptotically stable node while (D=$\frac{g-r}{g}$, w=0) is an unstable star node.

A3 Case III – Synthesized Optimal Control

As discussed above, when a synthesized optimal control is optimal, a singular control will also lead the whole system into an equilibrium. We will derive the singular path and analyze the characteristics of the equilibria driven by the singular path in this case. In our model, the singular path results in two potential equilibria. Both theoretical analysis and numerical simulation show that one of the potential

steady states is an unstable star node, while the other is a saddle point. Detailed discussion is shown in the following. In the following, I will first solve for the singular path. Then I will turn to analyzing the characteristics of the equilibria driven by the singular path, numerically and analytically.

Solving for the singular path involves investigating conditions that must hold when the switching function is identically zero for some finite interval. If the switching function, $\sigma(t)$, is zero, then its derivative must also be zero. Differentiating the switching function gives us:

$$\frac{d\sigma}{dt} = -\lambda whD\left[\frac{d\lambda/dt}{\lambda} + \frac{dw/dt}{w} + \frac{dD/dt}{D}\right] + \mu hw(w-1)\left[\frac{d\mu/dt}{\mu} + \frac{dw/dt}{w}\right] + \mu hw^2 \frac{dw/dt}{w} \quad \text{(A3-5)}$$

We also know from the Pontryagin conditions that the adjoint variables must satisfy:

$$\rho\lambda - \frac{d\lambda}{dt} = \frac{dH}{dD} = \alpha + \lambda[g(1 - 2*D) - wqh - (1-w)r] \quad \text{(A3-6)}$$

and

$$\rho\mu - \frac{d\mu}{dt} = \frac{dH}{dw} = -\lambda[qhD - rD] + \mu(qh - r)(2w-1) \quad \text{(A3-7)}$$

From (A3-6) and (A3-7), it can be shown that:

$$\frac{d\lambda/dt}{\lambda} + \frac{dD/dt}{D} = \rho - \frac{\alpha}{\lambda} + gD \quad \text{(A3-8)}$$

$$\frac{d\mu/dt}{\mu} + \frac{dw/dt}{w} = \rho - \left(w - \frac{\lambda D}{\mu}\right)*(qh - r) \quad \text{(A3-9)}$$

Substituting (A3-8), (A3-9), $\frac{dw}{dt}$, and $\frac{dD}{dt}$ into the expression for the rate of change of the switching function (A3-5), we have:

$$\frac{d\sigma}{dt} = -\lambda whD*\left[\frac{d\lambda/dt}{\lambda} + \frac{dD/dt}{D}\right] + \left[\frac{dw/dt}{w}\right]*(\mu hw^2 - \lambda whD)$$

$$+ \mu hw(w-1)[\ \frac{d\mu/dt}{\mu} + \frac{dw/dt}{w}\ ]$$

$$= -\lambda whD * [\rho - \frac{\alpha}{\lambda} + \frac{gD}{K}] \quad + \quad [\frac{dw/dt}{w}]*(\mu hw^2 - \lambda whD) +$$

$$+ \mu hw(w-1)[\ \rho - (\frac{\lambda D}{\mu} + w)*(qh-r)] \qquad \text{(A3-10)}$$

Expanding this gives us:

$$\frac{d\sigma}{dt} = -\rho[\lambda whD - \mu hw(w-1)] + whD\alpha - \lambda whD*gD \qquad \text{(A3-11)}$$

With the switching function, it can be shown that the terms inside the first bracket in (A3-11) equals to c. So, the equation (A3-5) becomes

$$\frac{d\sigma}{dt} = -\rho c + whD\alpha - \lambda whD*\frac{gD}{K} = 0 \qquad \text{(A3-12)}$$

Since the switching function is zero along the singular interval, its first derivative also must be zero and hence the above equation (A3-12) must hold. For the same reason, it second derivative of the switching function also must be zero, or

$$\frac{d(d\sigma/dt)}{dt} = whD\alpha\ [\frac{dw/dt}{w} + \frac{dD/dt}{D}]$$

$$- \lambda whD*\frac{gD}{K}\ [\frac{d\lambda/dt}{\lambda} + \frac{dw/dt}{w} + 2*\frac{dD/dt}{D}] \qquad \text{(A3-13)}$$

Substituting $\frac{d\lambda/dt}{\lambda} + \frac{dD/dt}{D} = \rho - \frac{\alpha}{\lambda} + gD$, and the two co-state equations into Equation (A3-13), and collecting terms, we get:

$$\frac{d(d\sigma/dt)}{dt} = whD(\alpha - \lambda gD)*(\frac{dw/dt}{w} + \frac{dD/dt}{D}) - \lambda whD*gD*(\rho - \frac{\alpha}{\lambda} + gD) \qquad \text{(A3-14)}$$

Since Equation (A3-14) equals zero, dividing whD on both sides and inserting the state equation for $\frac{dw/dt}{w}$ and $\frac{dD/dt}{D}$ yields:

$$\frac{\rho c}{whD} *[(qh -r) (w-1) + g(1- D) – wqh – (1-w)r \quad + \rho + gD] - \alpha\rho =0 \qquad \text{(A3-15)}$$

$$\text{Or} \qquad q^{\text{singular control}} = \frac{\rho + g}{h} \quad - \quad \frac{\alpha wD}{c} \qquad \text{(A3-16)}$$

This equation must be satisfied along the singular path. In the following, I turn to analyzing the characteristics of the equilibria driven by the singular path. I will first solve for the possible steady states.

As discussed above, if the equilibrium is driven by a singular path, then, at the equilibrium, these following conditions must hold:

$$\frac{dD}{dt} \quad = gD(1 - D) – qwhD - (1-w)rD =0$$

$$\frac{dw}{dt} \quad = (qh – r)w(w-1) =0$$

$$\sigma (t) \quad = c - \lambda whD + \mu hw(w-1) \quad =0 \qquad \text{(A3-17)}$$

We also need to note that since the second order necessary conditions of a minimum do not hold (see Appendix 2), solutions of function system (A3-17) are not “real” steady states. We call these solutions, in this sense, “potential steady states”.

From the Pontryagin conditions of the Hamiltonian, we know that the adjoint variables must satisfy: $\rho\lambda - \frac{d\lambda}{dt} = \frac{dH}{dD} = \alpha + \lambda[g(1-2D) – wqh – (1-w)r]$. At the steady state, $\frac{d\lambda}{dt} = 0$, and $\frac{dD}{dt} = 0$. Therefore, we have $\rho\lambda = \alpha + \lambda[g(1- 2D) – wqh – (1-w)r] = \alpha + \lambda[\frac{dD}{dt} - gD] = \alpha - \lambda gD$. Solving this equation, we get $\lambda = \frac{\alpha}{\rho + gD}$. Similarly, another Pontryagin condition that the adjoint variables must

satisfy is that ρμ - $\frac{d\mu}{dt}$ = $\frac{dH}{dw}$ = λ[– qhD + rD] + μ(qh -r) (2w-1)= (qh -r)*[μ(2w-1) - λD]. Solving this question, we get $u = \frac{(qh-r)\lambda D}{w(qh-r)-\rho} = \frac{(qh-r)D*\frac{\alpha}{\rho+gD}}{w(qh-r)-\rho}$.

Plugging λ and μ into the switching function, we have σ (t) = c-whD* $\frac{\alpha}{\rho+gD}$ + hw(w-1)* $\frac{(qh-r)D*\frac{\alpha}{\rho+gD}}{w(qh-r)-\rho}$ =0. Now, the original function system (A3-17) becomes,

$\frac{dD}{dt}$ = gD(1 - D) – qwhD - (1-w)rD =0

$\frac{dw}{dt}$ = (qh – r)w(w-1) =0

σ (t) = c-whD* $\frac{\alpha}{\rho+gD}$ + hw(w-1)* $\frac{(qh-r)D*\frac{\alpha}{\rho+gD}}{w(qh-r)-\rho}$ =0 (A3-18)

From $\frac{dw}{dt}$ = (qh – r)w(w-1) =0, we can get three solution: w=0, w=1, and q=$\frac{r}{h}$.

First of all, if we plug q=$\frac{r}{h}$ into $\frac{dD}{dt}$ =0, we get two solutions: D_1 =0 and D_2 =$\frac{g-r}{g}$. Next, plugging q = $\frac{r}{h}$ and D=0 into the switching function, we get σ (t) = c-whD* $\frac{\alpha}{\rho+gD}$ + hw(w-1)* $\frac{(qh-r)D*\frac{\alpha}{\rho+gD}}{w(qh-r)-\rho}$ =c $\neq 0$. In other words, (q = $\frac{r}{h}$, D=0) can not be a steady state. However, if we plug another solution q = $\frac{r}{h}$ and D=$\frac{g-r}{g}$

into the switching function, we get w = $\frac{cg(\rho+g-r)}{ha(g-r)}$, which is a possible solution.

So the first potential steady state is (q= $\frac{r}{h}$, D=$\frac{g-r}{g}$, and w =$\frac{cg(\rho+g-r)}{ha(g-r)}$).

Secondly, if we plug w=0 into $\frac{dD}{dt}$=0, we get D_1 = 0 and D_2 =$\frac{g-r}{g}$.

However, if we plug in w=0 into the switching function, we get σ (t) = c - λwhD + uhw(w-1) = c $\neq 0$, no matter what D is. In other words, w=0 can not be a possible steady state.

Finally, if we plug w=1 into $\frac{dD}{dt}$=0, we get two solutions: D_1 = 0 and D_2 =$\frac{g-qh}{g}$. Then, we plug w=1 and D=0 into the switching function to get σ (t) = c - whD*$\frac{\alpha}{\rho+gD}$ + hw(w-1)* $\frac{(qh-r)D*\frac{\alpha}{\rho+gD}}{w(qh-r)-\rho}$=c $\neq 0$. So w=1 and D=0 can not be a possible steady state. However, if we plug w=1 and D=$\frac{g-qh}{g}$ into the switching function, we get σ (t) = c - whD*$\frac{\alpha}{\rho+gD}$ + hw(w-1)* $\frac{(qh-r)D*\frac{\alpha}{\rho+gD}}{w(qh-r)-\rho}$ = c – h*$\frac{g-qh}{g}$ *$\frac{\alpha}{\rho+g-qh}$. Solving this equation by setting σ (t) =0 yields $q=\frac{h\alpha g-cg(\rho+g)}{h^2\alpha-cgh}$. Finally if we plug this solution back into D=$\frac{g-qh}{g}$, we get $D=\frac{c\rho}{h\alpha-cg}$. So the second possible steady state is ($q=\frac{h\alpha g-cg(\rho+g)}{h^2\alpha-cgh}$, $D=\frac{c\rho}{h\alpha-cg}$, and w=1). Let us call these two possible stead states as points PSS1 and PSS2 respectively (Figure A4). In the following, I will first discuss the characteristics of these possible steady states both analytically. Then I will check the analytical results using numerical simulations.

In order to analytically discuss the characteristics of these two possible steady points, I will draw a phase diagram in a (D, w) plane. If we plug the singular path (A3-16), or $q^{\text{singular control}} = \frac{\rho+g}{h} - \frac{\alpha w D}{c}$, into the equation of motion $\frac{dD}{dt} =$ gD(1 - D) – qwhD - (1-w)rD , and $\frac{dw}{dt} = (qh - r)w(w-1)$, we get:

$$\frac{dD}{dt} = gD(1-D) - (\rho + g - \frac{\alpha h}{c} wD)wD - (1-w)rD$$

$$\frac{dw}{dt} = (\rho + g - r - \frac{\alpha h}{c} wD)w(w-1) \qquad \text{(A3-19)}$$

The phase diagram is determined by the equation system (A3-19).

First of all, to solve for the w and D nullclines, we set

$\frac{dw}{dt} = (\rho + g - r - \frac{\alpha h}{c} wD)w(w-1) = 0$, and $\frac{dD}{dt} = gD(1-D) - (\rho + g - \frac{\alpha h}{c} wD)wD - (1-w)rD = 0$.

Solving these two equations yields w=0, w=1, and $w = \frac{c*(\rho+g-r)}{\alpha h D}$; D=0, and

$D = \frac{g - (\rho+g)w - (1-w)r}{g - \frac{\alpha h w^2}{c}}$. These nullclines are plotted in Figure A4, which presents the phase portrait of the dynamic system.

Note that the nullclines divide the phase space into different isosectors. In the following, we will turn to the derivation of the vector field. In other words, we need to figure out the directions of motion for points not on the nullclines. First of all, we take the first derivative of $\frac{dD}{dt}$ with respect to w, and evaluate it at $\frac{dD}{dt} = 0$, we get

$$\left.\frac{dD/dt}{dw}\right|_{\frac{dD}{dt}=0} = -(\rho+g)D - \frac{\alpha h}{c} 2wD^2 + rD = D*[-(\rho+g)D - \frac{\alpha h}{c} 2wD + r] \qquad \text{(A3-20)}$$

The sign of $\left.\frac{dD/dt}{dw}\right|_{\frac{dD}{dt}=0}$ depends on the magnitude of w and D. Using the default value from Table 1, we can determine its sign numerically at the two steady states. If we plug the values of these two potential steady states (PSS1 and PSS2), the sign of $\left.\frac{dD/dt}{dw}\right|_{\frac{dD}{dt}=0}$ is positive at the first potential steady state (PSS1), with a high pest population and a relatively low fraction of susceptible pests, and its sign is negative at the second potential steady state (PSS2), with a small pest population and a maximum fraction of susceptible pests.

Similarly, by taking the first derivative of $\frac{dw}{dt}$ with respect to D and estimating it at $\frac{dw}{dt}=0$, we have:

$$\left.\frac{dw/dt}{dD}\right|_{\frac{dw}{dt}=0} = -\frac{\alpha h}{c} w * w * (w-1) \qquad \text{(A3-21)}$$

It is easy to see that $\left.\frac{dw/dt}{dD}\right|_{\frac{dw}{dt}=0}$ will be positive as long as w is less than 1, and it is negative when w is greater than 1. In other words, its sign is positive near the first potential steady state, and it is negative near the second potential steady state.

From the signs of $\left.\frac{dw/dt}{dD}\right|_{\frac{dw}{dt}=0}$ and $\left.\frac{dD/dt}{dw}\right|_{\frac{dD}{dt}=0}$, we can determine the direction of motions for points that are not on the nullclines (See Figure A4). In addition, numerical simulation of function A3-5 is consistent with the theoretical analysis above (Figure A5). Figure A5 shows that the equilibrium driven by the singular path is a saddle point.

Reference

Caprio, M.A., 1998. "Evaluating Resistance Management Strategies for Multiple Toxins in the Presence of External Refuge", *Journal of Economic Entomology,* Vol. 91, pp.1021-1031.

Clark, C. W. 1976. Mathematical Bioeconomics: The Optimal Management of Renewable Resources. New York, John Wiley & Sons, Inc.

Clive, J., 2003. "Global Status of Commercialized Transgenic Crops: 2003". The International Services Acquisition of Agri-Biotech Applications (ISAAA) Brief No.30: Preview. ISAAA, Ithaca, NY.

Gersvitz M., and J. Hammer, 2004. "The economical control of infectious diseases." *The Economic Journal* 114:1-27.

Gould, F., 1998. "Sustainability of transgenic insecticideal cultivars: integrating pest genetics and ecology", *Annual Review of Entomology*, pp.701-722.

Huang J.K., R.F. Hu, S. Rozelle, F.B. Qiao and C.E. Pray, 2002. "Small holders, Transgenic Varieties, and Production Efficiency: The Case of Cotton Farmers in China", *Australian Journal of Agricultural and Resource Economics*, Vol. 46. No. 3, pp. 367-387.

Hueth, D., U. Regev. 1974. "Optimal Agricultural Pest Management with Increasing Pest Resistance", *American Journal of Agricultural Economics*, Vol.56, pp.543-553.

Hurley, T.M., S. Secchi, B.A. Babcocak, and L. Hellmich, 1999. "Managing the risk of European corn borer resistance to Transgenic corn: An assessment of refuge recommendations", Staff Report 99 SR 88, February 1999. Center for Agricultural and Rural Development, Iowa State University, Ames, IA.

Judd, Kenneth L. 1998. Numerical Methods in Economics. Cambridge, MA: MIT Press.

Kelly, D., 2000. "Ingrad's resistance, refuge and planted areas," http://www.gene.ch/genet/2000/Dec/msg00006.html

Laxminarayan, R. and G. Brown, 2001. "Economic of Antibiotic Resistance: A Theory of Optimal Use", *Journal of Environmental Economic and Management*, Vol. 42, no,2, pp.183-206.

Laxminarayan, R. and R.D. Simpson, 2002. "Refuge strategy for managing pest resistance in transgenic agricultural", *Environment and Resource Economics*, Vol. 22, pp.521-536.

Li, G.P., K.M. Wu, F. Gould, H.Q Feng, Y.Z. He and Y.Y. Guo, 2002. "Bt toxin resistance gene frequencies in Helicoverpa armigera (hubner) population from the Yellow River cotton farming region of China". Research on Cotton Bollworm in China, (Yuyuan Guo, editor), Beijing, China.

Livingston, M.J., G.A. Carlson and P.L. Fackler, 2004. "Managing Resistance Evolution in Two Pests to Two Toxins with Refugia", *American Journal of Agricultural Economics*, Vol 86, no.1, pp.1-13.

Pray, C.E., D.M Ma, J.K. Huang and F.B. Qiao, 2001. "Impact of BT Cotton in China," *World Development*, Vol. 29, no. 5, pp. 813-825.

Pray, C.E., J.K. Huang, R.F. Hu, S. Rozelle, 2002. "Five years of Bt cotton in China - the benefits continue", *The Plant Journal*, Vol. 31, no.4, pp.423-430.

Ru L.J., J.Z. Zhao, and C.H. Rui, 2002. "A simulation model for adaptation of cotton bollworm to transgenic Bt cotton in Northern China", *Acta Entomologica Sinica*, Vol.45, no.2, pp. 153-159.

Secchi S., Terrance M. Hurley, and R.L. Hellmich, 2001. "Managing European Maize Borer Resistance to Bt Maize with Dynamic Refuges", Working Paper, 01-WP 287, Center for Agricultural and Rural Development, Iowa State University, Ames, IA.

Storer, N.P., S.L. Peck, F. Gould, J.W. V. Duyn, and G.G. Kennedy, 2003. "Spatial Processes in the Evolution of Resistance in Helicoverpa zea (Lepidoptera: Noctuidae) to Bt Transgenic Corn and Cotton in a Mixed Agroecosystem: a Biology-rich Stochastic Simulation Model", *Journal of Economic Entomology*, Vol.96, no.1, pp.156–172.

Traxler, G., S. Godoy-Avila, J. Falck-Zepeda and J. Espinoza-Arellano, 2001. "Transgeenic cottin in Mexico: economic and environmental impacts". Working Paper, Department of Agricultural Economics, Auburn University, Auburn, A.L.

Turner D., 2000. "No room for complacency on resistance to Bt," http://www.gene.ch/genet/2000/Dec/msg00006.html

Wilen, J.E., Siwa Msangi. 2002. Dynamics of Antibiotic Use: Ecological versus Interventionist Strategies to Management Resistance to Antibiotics". Battling Resistance to Antibiotics and Pesticides: An Economic Approach (Ramanan Laxminarayan, editor), pp. 18-41.

Wu, K.M., Y.Y. Guo, and W.G. Wang, 2000. "Field resistance evaluations of Bt transgenic cotton GK series to cotton bollworm", *Acta Phytophylacica Sinica*, Vol.27, no.4, pp. 317-321.

Xue, D.Y, 2002, "A summary of research on the environmental impact of Bt cotton in China", Greenpeace, June 2002.

Table 1: Parameters, sources and range for Bt-resistance and economic parameters explored in the sensitivity analysis

Parameter	Default	Source
Average yield loss due to pest	\$1030/ha	Calculated based on data collected by IPP[a]
Average Bt cotton planting cost	\$143/ha	Calculated based on data collected by CCAP[b]
Discount rate	0.036	0.1 (Livingston et al., 2002); 0.04 (Hurley et al., 2001)
Initial fraction of resistant pests	0.001	Personal talk with Kongming Wu
Mortality rate of susceptible pest in Bt field	0.90	0.85-0.95 (Wu et al., 2000); 0.75((Livingston et al., 2002); Storer et al. (2003); 0.95(Caprio, 2000)
Intrinsic growth rate	0.68	Author's Calculation

a. IPP is the Institute of Plant Protection of the Chinese Academy of Agricultural Science.
b. CCAP is the Center for Chinese Agricultural Policy (CCAP) of the Chinese Academy of Sciences (CAS).

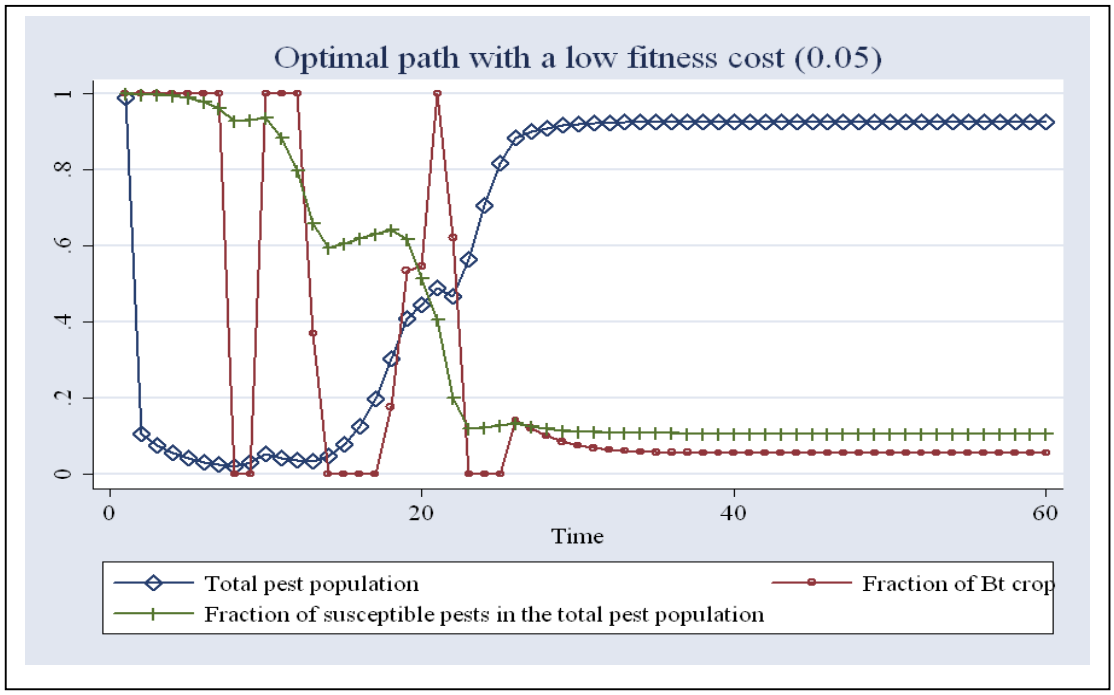

Panel A

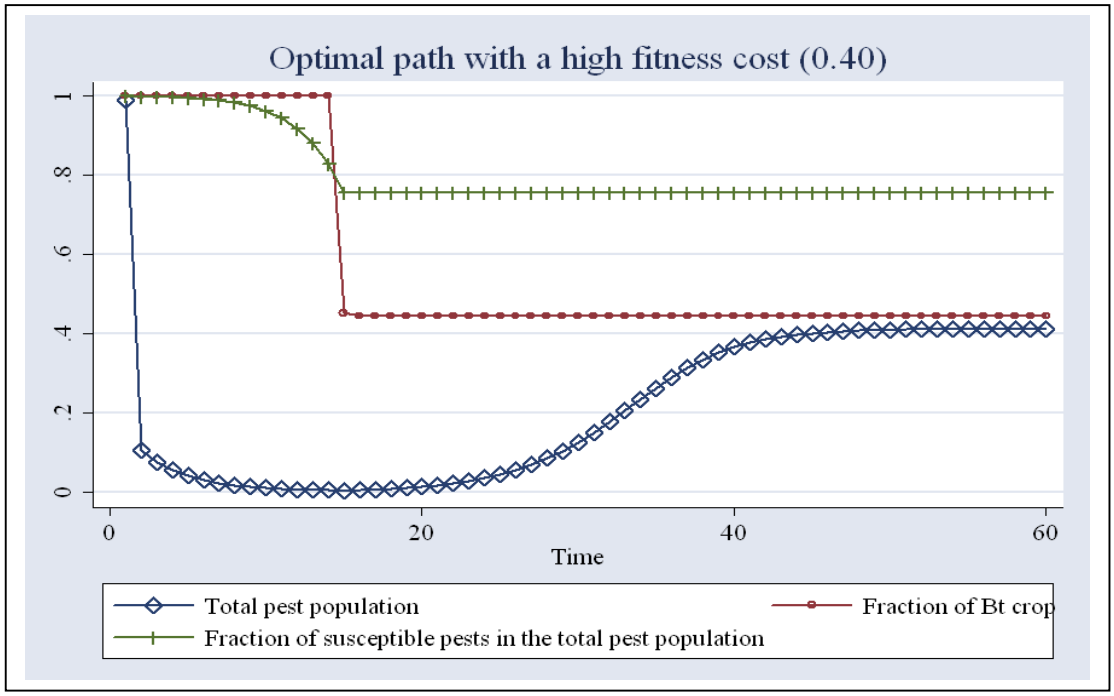

Panel B

Figure 1. Simulation results of the bioeconomic model

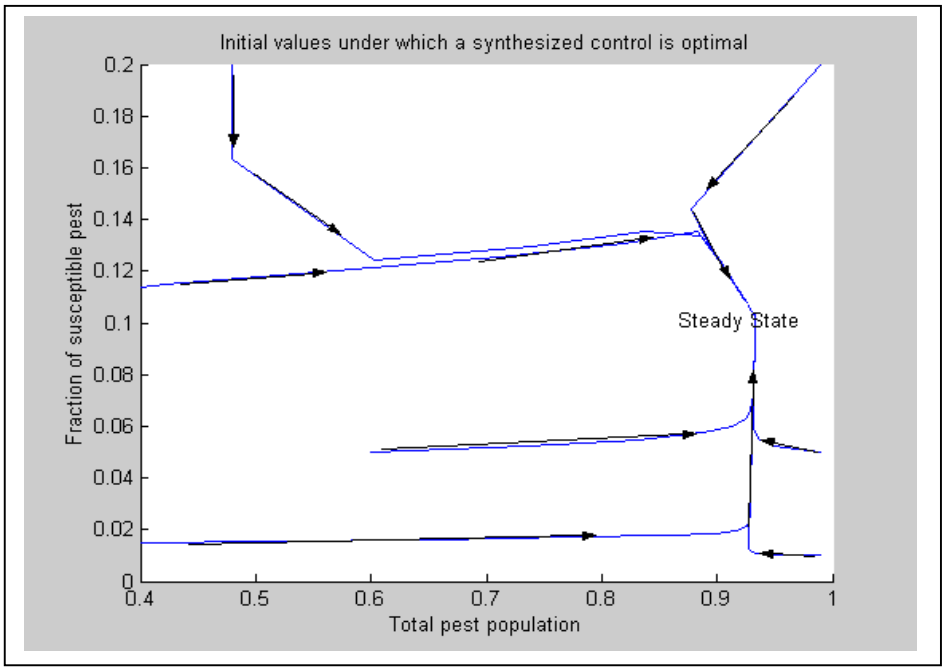

Panel A

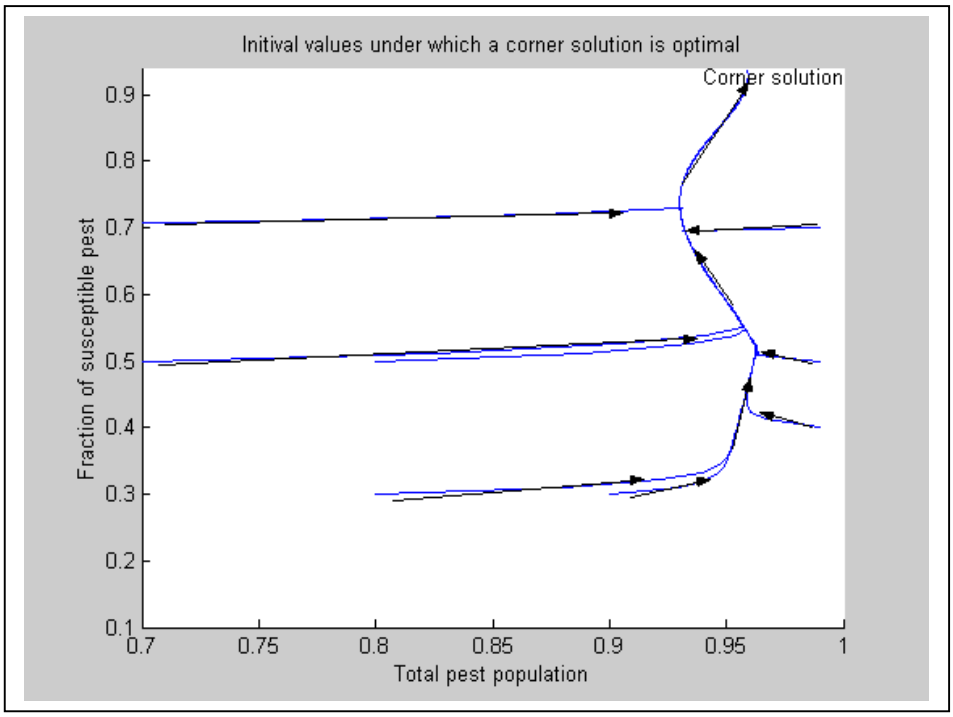

Panel B

Figure 2. Initial values and optimal control path

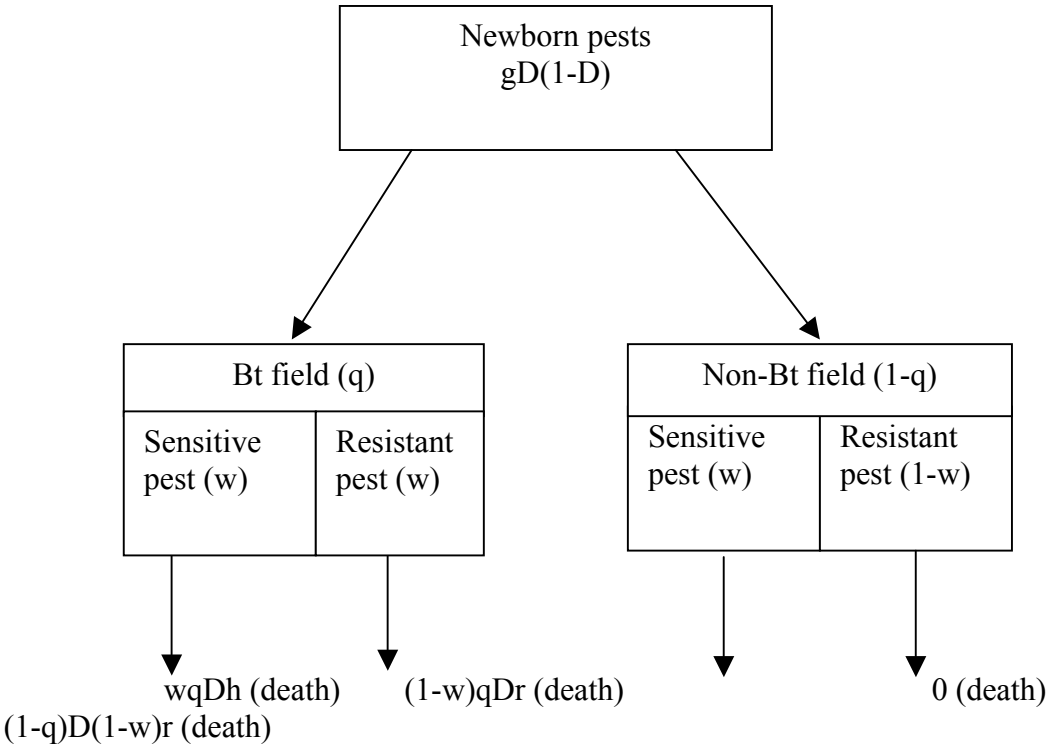

D: total pest population
g: an intrinsic growth rate
w: the proportion of susceptible pests in the population
q: fraction of Bt land
h: death rate of susceptible pests in Bt field
r: death rate of resistant pests in either Bt or non-Bt field

Figure A1. Schematic of the biological model with refuge

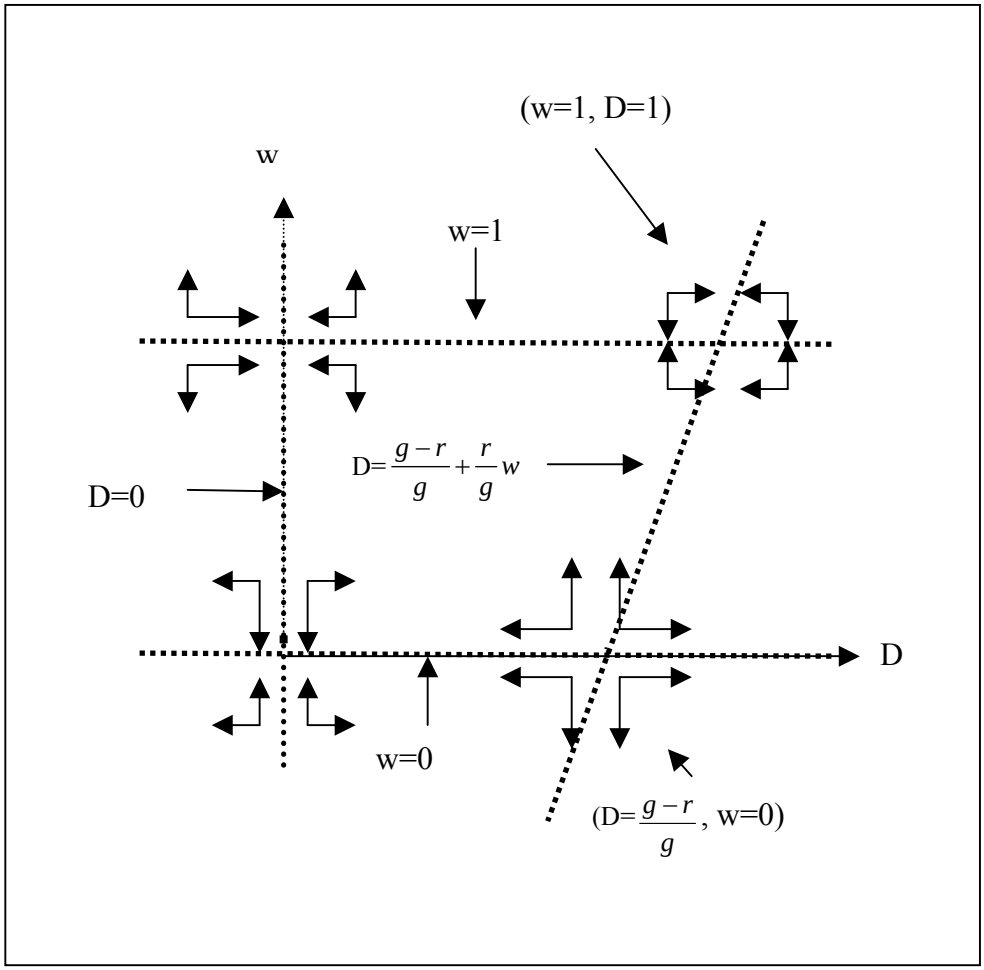

Figure A2. Phase diagram to show the characteristics of the four fixed points led by the no control strategy: (D=0, w=0) and (D=0, w=1) are two saddle points, (D=1, w=1) is an asymptotically stable node while (D=$\frac{g-r}{g}$, w=0) is an unstable star node.

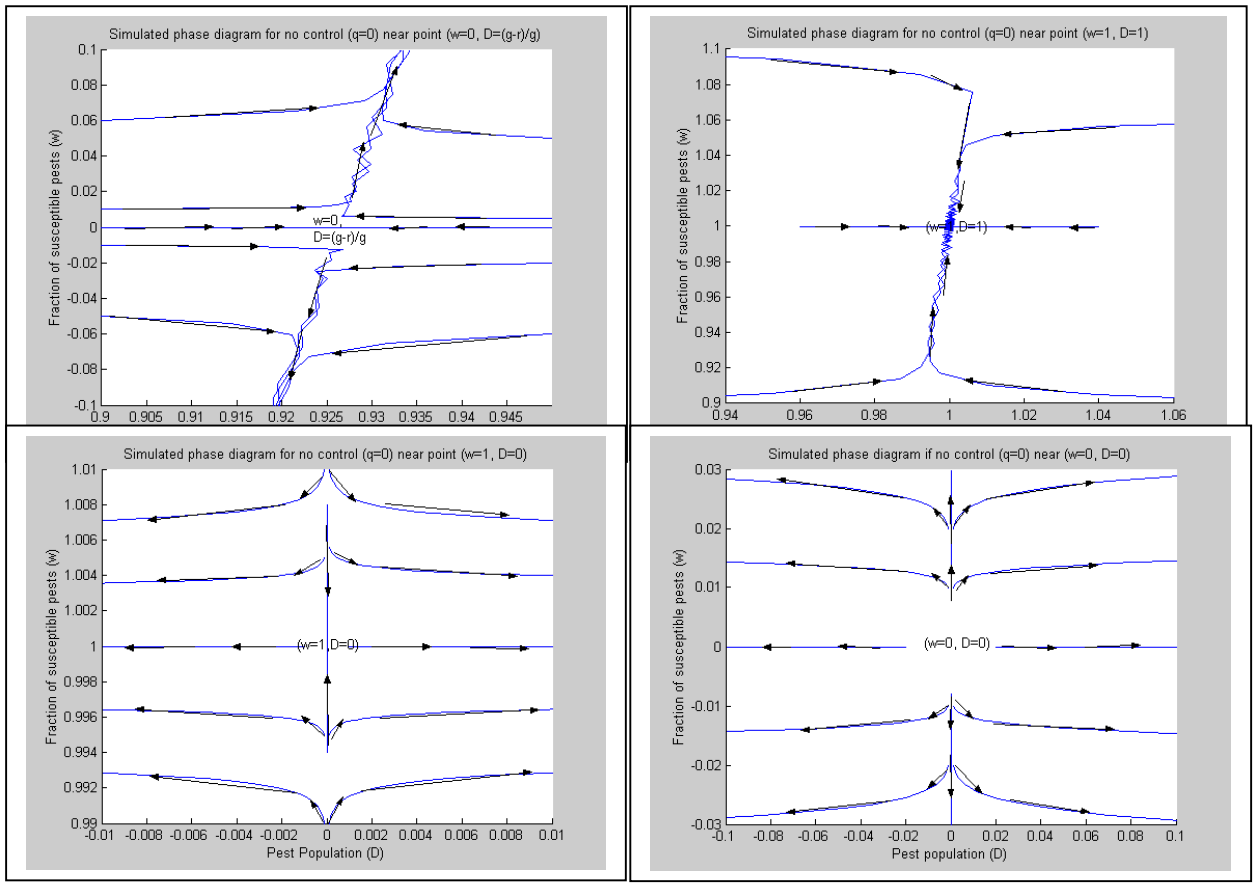

Figure A3. Numerical analysis of the characteristics of the four fixed points led by the no control strategy: (D=0, w=0) and (D=0, w=1) are two saddle points, (D=1, w=1) is an asymptotically stable node while (D=$\frac{g-r}{g}$, w=0) is an unstable star node.

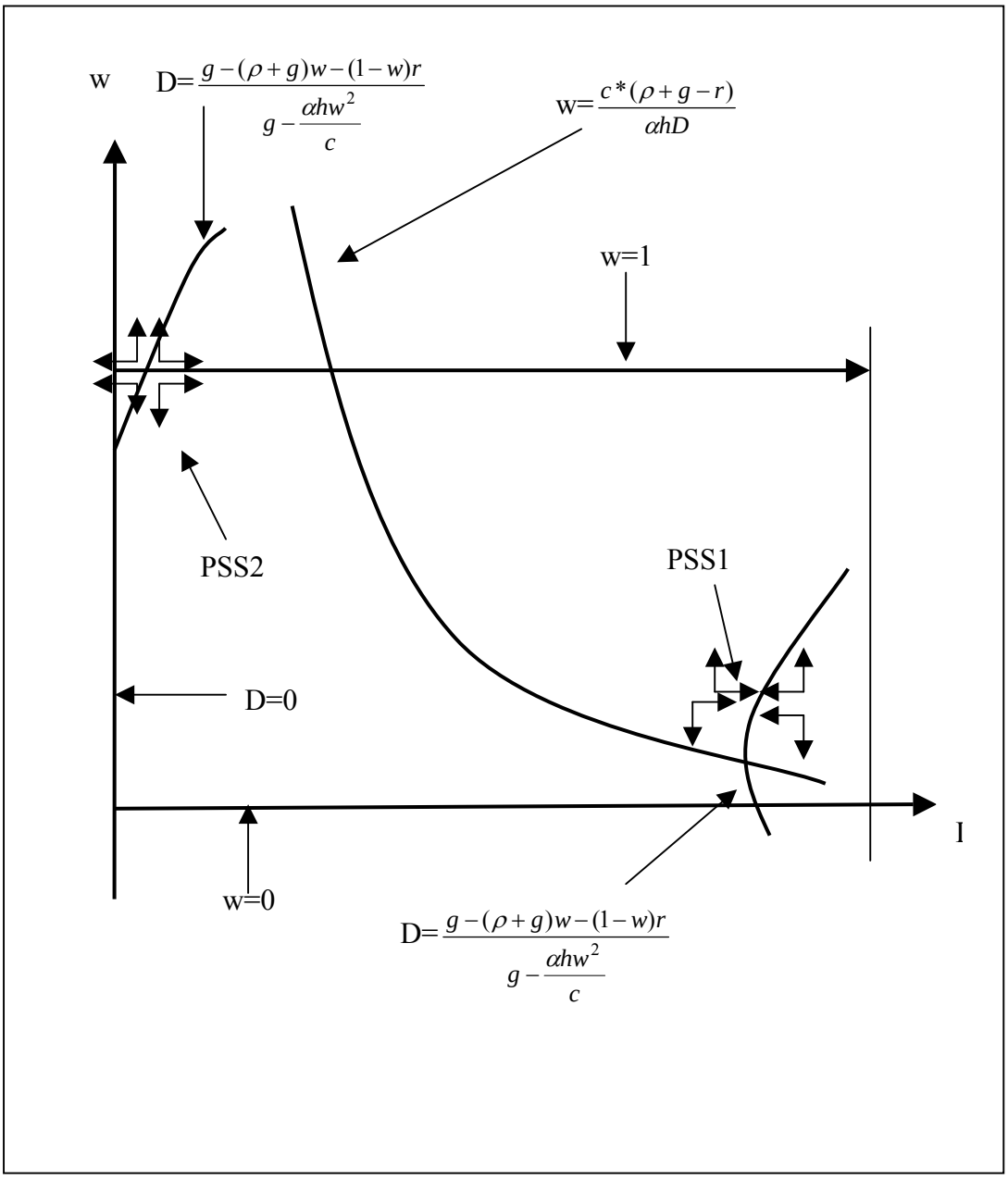

Figure A4. Phase diagram to show the characteristics of the two fixed points led by the singular path: ($D=\frac{c\rho}{h\alpha-cg}$, w=1) is a unstable star node, (D= $\frac{g-r}{g}$, w = $\frac{cg(\rho+g-r)}{ha(g-r)}$) is a saddle point.

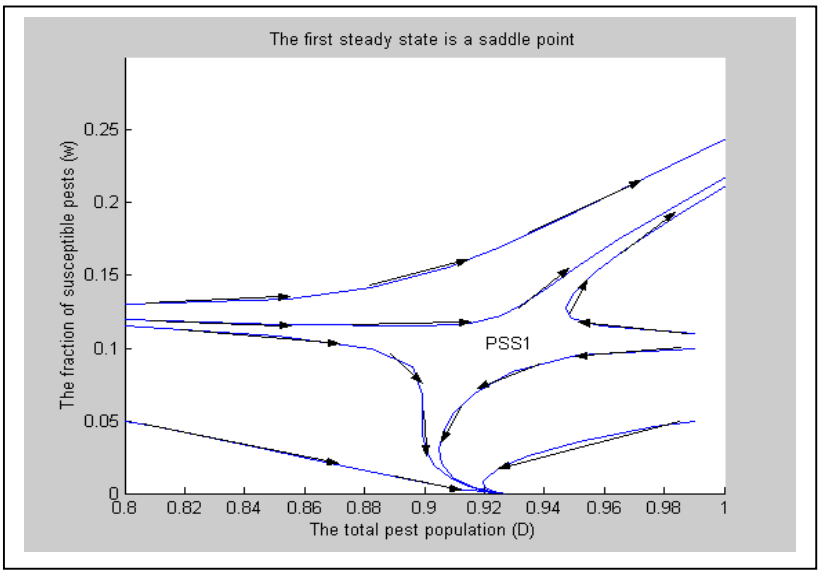

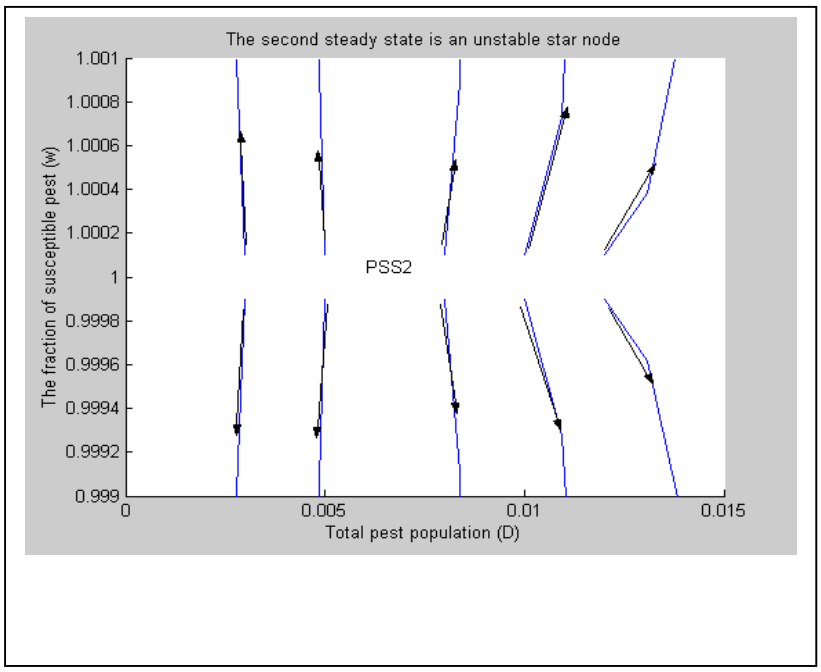

Figure A5. Numerical analysis of the characteristics of the two fixed points led by the singular path: ($D = \frac{c\rho}{h\alpha - cg}$, w=1) is an unstable star node, (D=$\frac{g-r}{g}$, w =$\frac{cg(\rho+g-r)}{ha(g-r)}$) is a saddle point.